Novel hybrid blade design and its impact on the overall and self-starting performance of a three-dimensional H-type Darrieus wind turbine

Yunus Celik[a,b,c*], Derek Ingham[a], Lin Ma[a], Mohamed Pourkashanian[a]

[a] *Energy2050, Department of Mechanical Engineering, Faculty of Engineering, University of Sheffield, United Kingdom*

[b] *Department of Mechanical Engineering, Faculty of Engineering, Hakkari University, Turkey*

[c] *Faculty of Science and Engineering, Swansea University, Bay Campus, Swansea, SA1 8EN, United Kingdom*

Abstract

The present study proposes a novel hybrid blade design that is the combination of a conventional airfoil, namely the NACA0018, and its J-shaped profile to increase the torque generation at the start-up stage of the turbine while decreasing the potential efficiency loss at the high tip speed ratios. Therefore, a new 2D-based design methodology was proposed, and depending on this methodology, different hybrid blade configurations were determined for the investigation of the overall and self-starting performance of the H-type Darrieus vertical axis wind turbine. Due to the inherent shape of the proposed hybrid blade, a 3D CFD dynamic start-up model, which is based on the fluid-turbine interaction, was built and used to evaluate the performance of the different configurations of the hybrid blades. The results indicate that although the proposed design methodology is based on the 2D-CFD calculations, it enables a quicker prediction of the aerodynamic performance of the proposed hybrid blades compared to the 3D-based CFD simulations. Furthermore, the findings also clearly illustrate that the new proposed hybrid blade designs not only overcome the self-starting issue of the turbine but also provide a wider turbine operating range and an improvement in the turbine peak efficiency in contrast to the losses caused by J-shaped airfoils.

Keywords

Hybrid blade design, Aerodynamics, Fluid-turbine interaction, Self-starting, Computational Fluid Dynamics (CFD), Vertical axis wind turbine

* Corresponding author. Department of Mechanical Engineering, Faculty of Engineering, Hakkari University, Hakkari, Turkey.

E-mail address: yunuscelik@hakkari.edu.tr

1. Introduction

The development and utilisation of renewable energy systems have a huge impact to mitigate global warming concerns that is a result of increasing pollution levels (Hand and Cashman, 2020; Zhao et al., 2022). Wind energy can be considered as one of the most cost-effective renewable energy systems, and it has undergone rapid expansion across the world. In recent years, there has been an increase in the usage of the vertical axis wind turbines (VAWTs) for small-scale power generation, in addition to the growing number of wind farms that include large horizontal axis wind turbines (HAWTs). However, the small-scale VAWTs, in particular the H-type Darrieus VAWTs, still suffer from the inherent low starting ability that is mainly due to weak torque generation at the low tip speed ratios (λ) (Celik et al., 2020; Khalid et al., 2022; McLean et al., 2022; Mohamed et al., 2021; Torabi et al., 2016; Zhu et al., 2015). Therefore, the deficiency of the self-starting of the H-type Darrieus VAWTs has been a popular topic among the researchers and several approaches, including active or passive pitching strategies, hybrid turbine designs, and modification on the turbine geometry such as camber, blade thickness, and turbine solidity, etc., have been used to overcome the self-starting issue (Abdolahifar and Karimian, 2022). Even though current approaches may enhance the turbine's ability to self-start, they can also lead to some serious issues, such as a noticeable loss in the power coefficient at the higher tip speed ratio region. Over the years, a considerable amount of research has been carried out improving the self-starting capability of the small-scale H-type Darrieus VAWTs by optimising various design parameters (Abdalrahman et al., 2022; Bhuyan and Biswas, 2014; Bianchini et al., 2015; Didane et al., 2019; Mitchell et al., 2021; Saad et al., 2021; Sengupta et al., 2016; Su et al., 2020; Sun et al., 2021; Tavallaeinejad et al., 2022). The literature survey clearly shows that the most reliable self-starting VAWT design can be achieved with either modification of the airfoil profile or design of the various configurations of the vertical axis wind turbine, for instance, the Hybrid VAWT. However, the present approaches have their own unique advantages and disadvantages.

A Hybrid VAWT consists of the H-type Darrieus turbine and the Savonius turbine that are lift-based and drag-based turbine utilised in tandem in the same turbine design. The main objective of the Hybrid turbine is to overcome the drawbacks of each turbine design, such as achieving the self-starting ability at low tip speed ratios and high power output at relatively high tip speed ratios. However, the Hybrid VAWT design has several problems, including new forms of vortex shedding leading to high losses, the complexity of the system design increasing the costs, etc. (Hosseini and Goudarzi, 2019). Gavaldà et al. (1990) examined the Savonius turbine contribution to the Hybrid turbine design and it has been found that the Savonius turbine provides an important benefit to the turbine self-starting capability under a wider variety of wind speeds and directions.

Gupta and Biswas (2011) have also carried out the numerical simulations to investigate the impact of the design parameters, in particular the overlap ratio and bucket size, on the hybrid VAWT design, which consists of eggbeater types of Darrieus turbine and a 3-blade Savonius turbine. For this purpose, various overlap ratios have been investigated at the tip speed ratio of 0.215 and 0.45. The maximum lift-to-drag ratio at low Reynolds numbers has been found to be reached with an overlap ratio of 16.2%. On the other hand, in terms of the start-up capability of the Hybrid VAWT design, Bhuyan and Biswas (2014) have analysed and compared the start-up requirements of the Hybrid VAWT and conventional H-type Darrieus VAWT. The findings show that an improved start-up capability has been achieved with the Hybrid VAWT design in comparison with the conventional H-type Darrieus VAWT at any azimuthal angle and Reynolds number. At higher wind speeds, the Savonius turbine, on the other hand, can operate as a brake for Hybrid VAWT designs, as a result the maximum power generation is reduced. Liang et al. (2017) carried out a computational analysis in order to achieve the optimum diameter ratio and the number of turbine blades for the Hybrid VAWT design, which consists of a Savonius rotor and Darrieus rotor as the internal and external, respectively. The research findings show that the Hybrid VAWT with an attachment angle of 0° and a 0.25 diameter ratio has been found to provide the optimum performance. In addition to this, while the tip speed ratio decreases, it has been observed that the overall efficiency and start-up torque generation have improved. Gao et al. (2022) proposed a drag-lift hybrid vertical axis wind turbine having the NACA0018 airfoil. In their design, the blade structure is adaptively changed during the rotation, therefore, while a drag shape is used under the low tip speed ratio region, a lift shape is used with the increase in the tip speed ratio. Thus, the overall performance of the turbine has been increased by trying to eliminate the deficiencies of both airfoils in a single blade. Asadi and Hassanzadeh (2022) examined the influence of the internal rotor types, namely semicircle and Batch-type, on the power performance of a hybrid vertical axis wind turbine, which consists of 2 straight blades. The findings indicate that while the internal rotor type has a considerable impact on the turbine performance, the Batch-type rotor was found to be superior to the semicircle rotor.

On the other hand, the modification of the airfoil profile has a significant influence on the turbine overall aerodynamic performance, as well as on its start-up characteristics. Recently, several efforts to modify the airfoil profile have been attempted (Dabiri, 2011; Dominy et al., 2007; Sheldahl and Klimas, 1981; Syawitri et al., 2022; Ullah et al., 2020; Wang et al., 2010; Yousefi Roshan et al., 2021). As an example of the modification of the airfoil, the J-shaped profile, which is designed by eliminating a portion of either the pressure or suction side, has been utilised to assist the turbine start-up ability by increasing the torque generation at the low tip speed ratios.

However, there are just a few studies existing in the literature that examine how the J-shaped airfoil affects the overall performance of the turbine, including the self-starting capability (Celik, 2021; Celik et al., 2022; Mohamed, 2019; Sun et al., 2020; Zamani et al., 2016a, 2016b). According to the literature review conducted, the turbine blade having the J-shaped profile was found to drastically reduce the turbine efficiency at high tip speed ratio values, even if it improves start-up performance as a consequence of the high torque output at low tip speed ratio values.

1.1. Research aims

The existing literature clearly demonstrates a need for another approach when the low starting torque capability and high performance loss at higher rotational speed conditions are taken into account. For this reason, for the first time, an alternative solution, which is called the Hybrid Blade design, is presented in the present study to not only enhance the self-starting efficiency of the lift-based H-type Darrieus VAWTs, but also maintain high efficiency at the normal operating conditions. A sketch of the one of the proposed Hybrid Blade designs is illustrated in Fig.1. In order to achieve this, a hybrid blade design methodology that can effectively combine a conventional airfoil, such as the NACA0018, and its J-shaped profile has been developed and proposed. The benefit of utilising the J-shaped airfoil, which has a large positive drag, in the hybrid profile design is to generate sufficient torque to start the turbine when it is needed and accelerate the turbine up to the point where the conventional airfoil becomes efficient. Furthermore, a series of high-fidelity 3D CFD simulations have been utilised, validated against the experimental study and previously obtained 2D CFD results, to evaluate the impact of the newly proposed hybrid design on the H-type Darrieus VAWT from both start-up and overall performance points of view. To the best of the authors' knowledge, the performance analyses of the turbine having such a proposed hybrid blade design have never been studied in the literature.

The objectives and novelty of the current work can be summarised as follows:

- For the simplicity and the faster computational analysis, a hybrid blade design methodology has been developed based on the 2D CFD simulations and the torque performance of the turbine with the proposed hybrid blade designs at the various tip speed ratios has been analysed.
- Different hybrid blade configurations that were thought to have a considerable impact on the self-starting performance of the turbine have been proposed. In contrast to the literature, the J-shaped profile was not utilised alone throughout the blade span, the J-shaped profile has been placed at either tip or middle of the blades by considering both the open and closed tips.

- Instead of using various constant rotational speeds of the turbine, a dynamic start-up model based on time-varying data was built and utilised in the simulations to assess the performance of the proposed hybrid blade designs by comparing with both the conventional and the J-shaped airfoils.

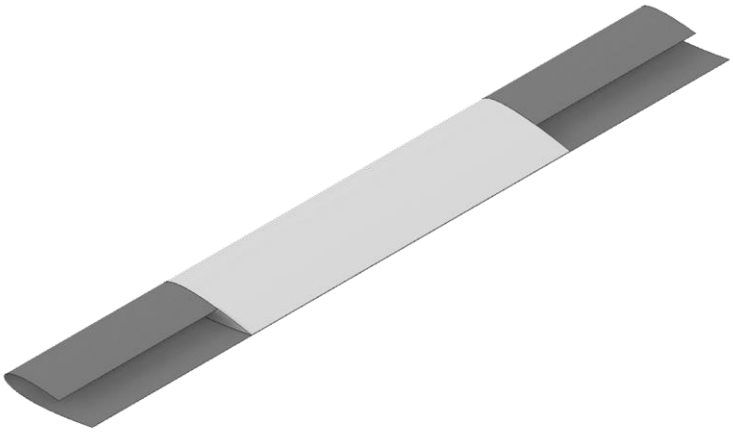

Fig. 1. Schematic of the one of the proposed Hybrid Blade designs having a conventional NACA0018 airfoil and its 40% opening J-shaped profile.

2. 3D CFD turbine modelling

Generally, most CFD studies have simplified the model into a two-dimensional analysis due to the straight characteristics of the H-type Darrieus VAWT blade because two-dimensional simulations are much simpler and faster compared to the three-dimensional simulations. Although the two-dimensional CFD model appears sufficient to evaluate the performance of the H-type Darrieus VAWT application with acceptable accuracy, two-dimensional simulations generally over-predict the overall performance since they neglect the spanwise secondary flow and vortices from the tip end (Zhang et al., 2019). In the present investigation, a full three-dimensional CFD dynamic start-up model, which is based on the fluid-turbine interaction, for the H-type Darrieus VAWT is required due to the inherent shape of the proposed hybrid blade design. For this reason, in the present study, a three-dimensional CFD model was built with new user-defined function (UDF) (see Appendix) after performing a mesh independency analysis to achieve a more realistic and reliable design. Furthermore, more detail on the calculations of the turbine dynamic start-up process can be found in the authors' previously published research paper (Celik et al., 2022).

2.1. Numerical settings and modelling strategies

A series of validation studies have been conducted in order to ensure the accuracy and reliability of the current 3D CFD start-up model and the findings were compared with the data from a published experiment conducted by Rainbird (2007). Based on the work of Rainbird, a 3-blade H-type Darrieus VAWT having a height (H) of 0.6m and a turbine radius (R) of 0.375m, has been simulated for the 3D CFD turbine validation study. Furthermore, the symmetrical NACA0018 airfoils having a 0.083m chord length (c) were used in the present studies.

The schematic of the three-dimensional computational domain used in the present study and boundary conditions are given in Fig. 2. For the present study, the geometry of the 3D computational domain has been obtained by extending the 2D CFD model, which was employed in the authors' previously published paper (Celik et al., 2020). In order to reduce the computational cost, only the upper half of the turbine has been considered in the numerical process since the flow around the hybrid blade experiences a symmetrical flow behaviour. To achieve this, a symmetrical boundary condition has been used at the bottom surface of the computational domain. The left-hand side of the computational domain has been considered as a velocity inlet under a fixed wind velocity of 6 m/s, which was selected according to the experimental study. Furthermore, a zero-gauge pressure-outlet boundary condition has been employed to the right-hand side of the computational domain. The SIMPLE scheme has also been applied to the pressure-velocity coupling using a gradient known as Green Node Based (Mazarbhuiya et al., 2020). The momentum and turbulence model equations are discretised using the second-order upwind scheme (ANSYS, 2013). The three-dimensional Reynolds-Averaged Navier-Stokes equations and the two-equation turbulence model SST $k-\omega$ have been employed in the present simulations (Almohammadi et al., 2015; Kaya et al., 2021; Naseem et al., 2020). A detailed discussion for the selection of the turbulence model can also be found in authors' previously published studies (Celik, 2021; Celik et al., 2020). Additionally, the residual convergence criterion has been set as 1×10^{-5} for all the variables.

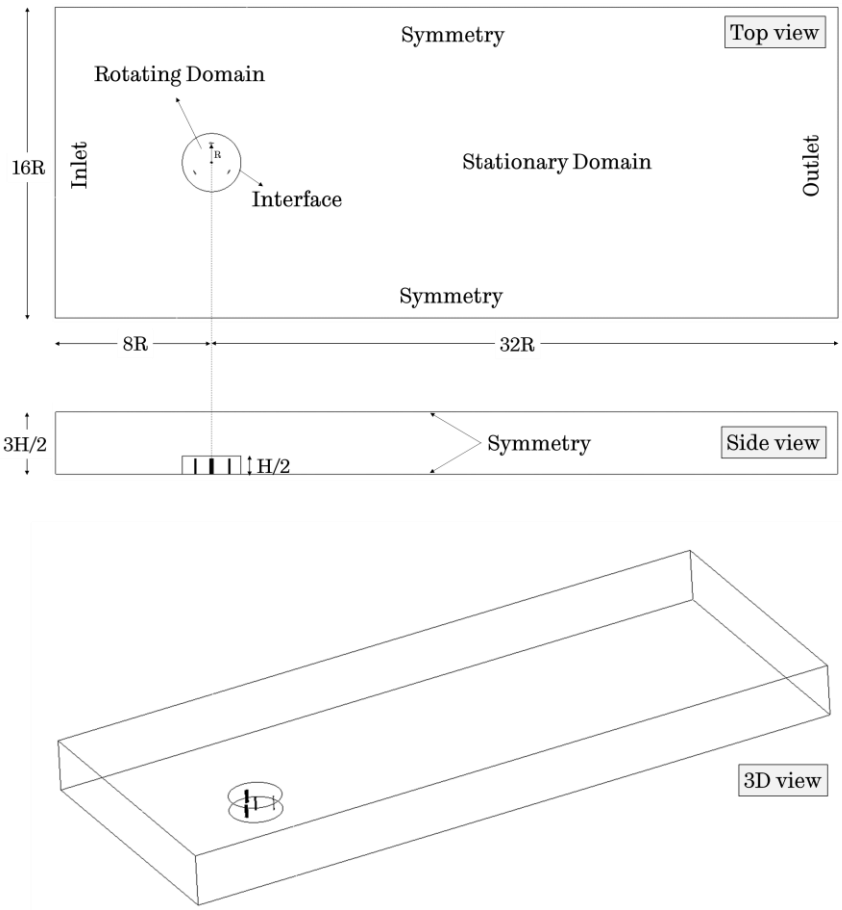

Fig. 2. Three-dimensional computational domain used in the present CFD calculations and the boundary conditions.

Furthermore, the time step is another factor, which influences the accuracy and efficiency of the CFD analyses. Thus, the time step size independency studies have been carried out using three different time step sizes, namely $\Delta t1 = 0.000144s, \Delta t2 = 0.00072s, and\ \Delta t3 = 0.00036s$, at the constant two different tip speed ratio values of 1.5 and 3. As Fig. 3 shows, the time step size of $0.00072s$ has been found to be sufficient, under the current numerical setup, considering the accuracy and computational efficiency, so it has been applied for the current time-varying dynamic start-up model verification studies and the further self-starting analyses of the hybrid blades. The time-step size selected is in a good agreement with the previous studies (Torabi et al., 2016). Furthermore, in the time-varying dynamic start-up simulations, it also results in an azimuthal increment per time step changing between the 0.000462° and 0.397° at the critical range of the tip speed ratio for the self-starting, which is between 0 and 1.5. This finding is also consistent with the study conducted by (Balduzzi et al., 2016).

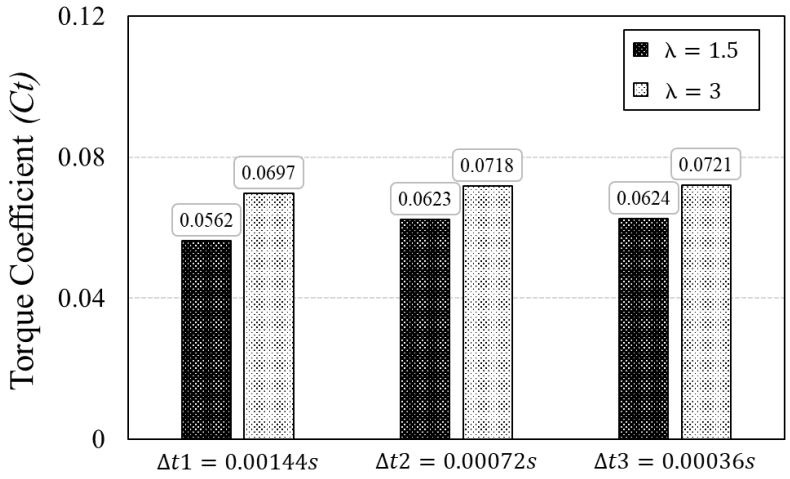

Fig. 3. Time step size independency analysis at tip speed ratios of 1.5 and 3.

2.2. Mesh independency analysis

Although the 3D CFD simulations of an H-type Darrieus VAWT can produce more accurate results compared to the 2D CFD simulations, the meshing and the calculation process take considerable time and effort. Therefore, conducting a mesh independency analysis is critical in order to select the proper number of meshes surrounding the airfoil in order to meet the calculation accuracy and computational cost requirements.

The 3D computational domain used in the present study consists of a rotating domain, where the turbine is located, and a stationary domain. As can be seen in the Fig. 4, structured mesh topologies have been applied to all the computational domains. In addition, the sliding mesh approach has been employed in order to consider the data exchange between these two adjacent domains with an interface boundary condition. The size of the meshes on the interface is consistent to ensure that the continuity, fast convergence, and accuracy of the CFD simulations are established. It is also important to note that two mesh domain files, namely stationary and rotating domains, have been created separately to simplify the meshing steps, and then, the generated meshes have been re-attached by using the appended function in the solver stage.

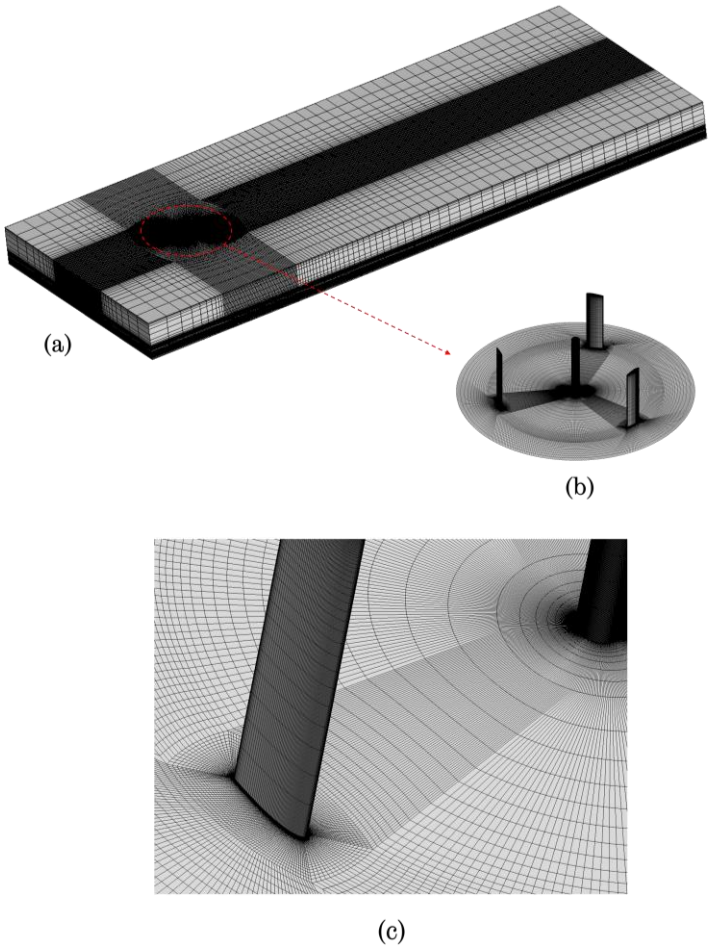

Fig. 4. Mesh configuration for the (a) stationary domain, (b) rotating domain, and (c) around the blade.

The mesh independency analysis has been conducted by using the three different sets of the nodes, i.e. Node 1, Node 2, and Node 3, as shown in Table 1. The baseline number of nodes (Node 2) has been selected based on the study conducted by (Zhang et al., 2019), and the same refinement factor has been applied to the calculation of the number of nodes for the coarse grid (Node 1) and fine grid (Node 3). The mesh size in the stationary domain has been kept the same during the refinement process that was applied to the meshes around the blades. Despite the fact that the number of meshes in the vicinity of the blade changes, the non-dimensional wall distance y^+ is maintained constant to reach the value that is recommended for enhanced wall treatment turbulence models (ANSYS Inc., 2014). In the current study, 30 mesh layers with the first cell height of about 4.5×10^{-5}m have been used to achieve a dimensionless y^+ value with an average $y^+ < 1$ maximum value of 2.5 (ANSYS Inc., 2014; Yagmur and Kose, 2021). Additionally, 60 spanwise mesh divisions have been employed to the blade half-length, which is consistent with the study by (Zhang et al., 2019). Fig. 5 illustrates the comparison of the results on the torque coefficient of the turbine obtained from a single turbine revolution considering the various number

of nodes at λ of 1.5 and 3 values. As can be seen from the figures, the torque coefficient obtained by Node 2 and Node 3 are very close at both λ values while Node 1 is different, especially at λ=1.5. Consequently, Node 2 can be selected confidently for further simulations, ensuring not only the computational correctness but also avoiding any additional computational costs.

Table 1. The different nodes used for the mesh independency analysis.

Nodes	Number of nodes around the blade 2D profile	Number of elements
Node 1	128	2,198,956
Node 2	184	3,161,265
Node 3	280	4,679,448

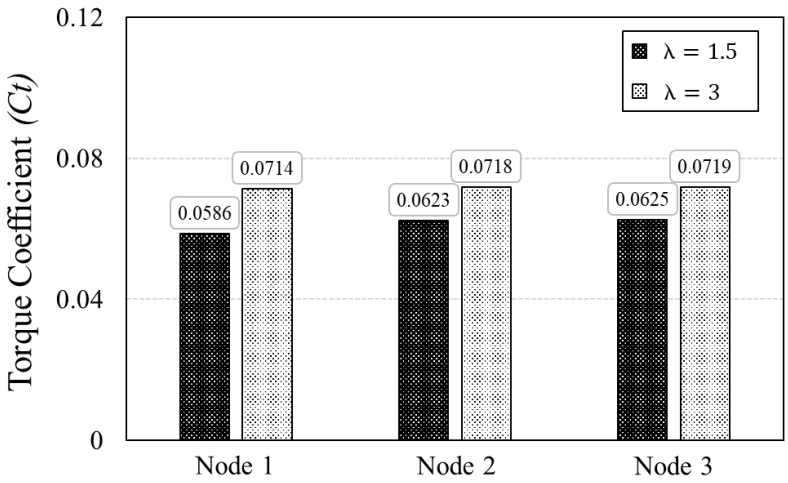

Fig. 5. Mesh independency analysis at tip speed ratios of 1.5 and 3.

2.3. 3D model verification

Fig. 6 shows the current 3D CFD simulation result with comparisons with the experimental data of Rainbird (2007) and the previously obtained 2D CFD model result in the author's previous study (Celik et al., 2020). The present 3D CFD model is capable of predicting the self-starting characteristics of the H-type Darrieus wind turbine investigated, as illustrated in the figure. It is also worth noting that the non-dimensional time axis defined as t/T (T is the time when the turbine reaches the steady-state condition) has been used to make the easier comparison between current CFD findings and experimental data. Although the experiment and the 2D CFD simulation required 150s and 15s, respectively, it has been found that the present 3D CFD simulation required approximately 31s to achieve the steady-state condition. Furthermore, the deviation in the λ values between the current 3D CFD prediction and the experimental study at steady-state conditions has

been obtained to be approximately 8.5%, while the difference between the 2D CFD prediction and the experimental study is 22%. The discrepancy between the 3D CFD and experimental study is assumed to be because of the absence of additional negative torque sources that were not incorporated in the current 3D models, such as the bearings and supporting arms. Nonetheless, when compared to the 2D CFD models, the 3D CFD analysis is able to provide valuable insight into the fluid dynamics of the self-starting stages of the H-type Darrieus wind turbine and is able to make a more precise estimation of the self-starting. For this reason, the current 3D CFD model setup can be used, with confidence, to evaluate the influence of the proposed hybrid blades on the aerodynamic performance and the self-starting behaviour of the H-type Darrieus VAWT.

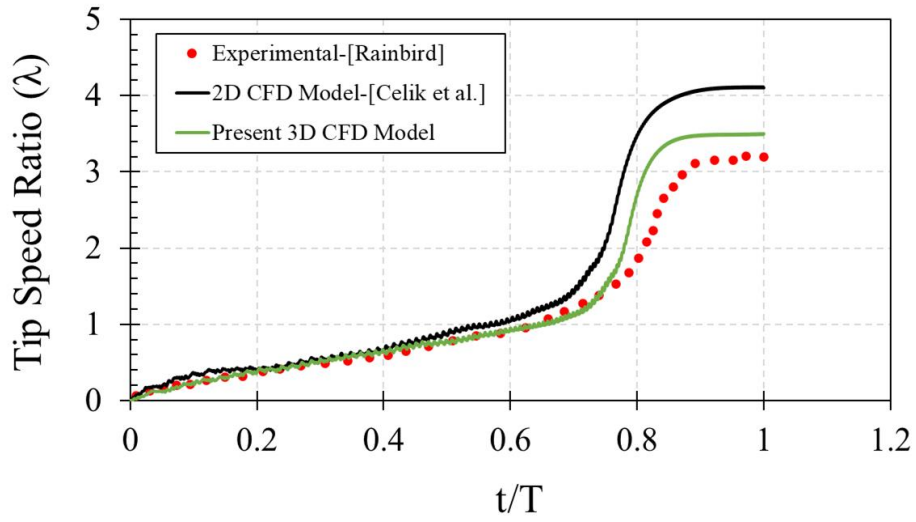

Fig. 6. The result of the dynamic start-up process from the current 3D CFD model in comparison with the experiment (Rainbird, 2007) and previously obtained 2D CFD result (Celik et al., 2020).

3. The philosophy of the design

As previously mentioned, the primary objective of the present work is to design, simulate, and evaluate the performance of the proposed hybrid blade design for self-starting H-type Darrieus VAWT. From this perspective, the philosophy of the design employed with the innovative hybrid blade design is explained in this section. It is also important to emphasise that in the current design process, as in the 3D CFD modelling process, the same turbine configuration has been used; however, the constant free wind speed of 5 m/s has been employed since it has been found in the authors' previous study (Celik et al., 2022) that the turbine does not self-starting under this circumstance. Therefore, the optimised hybrid blade design will make the turbine self-start under these circumstances. The procedure of the proposed hybrid blade design consists of three main design steps, which are systematically summarised in Fig. 7.

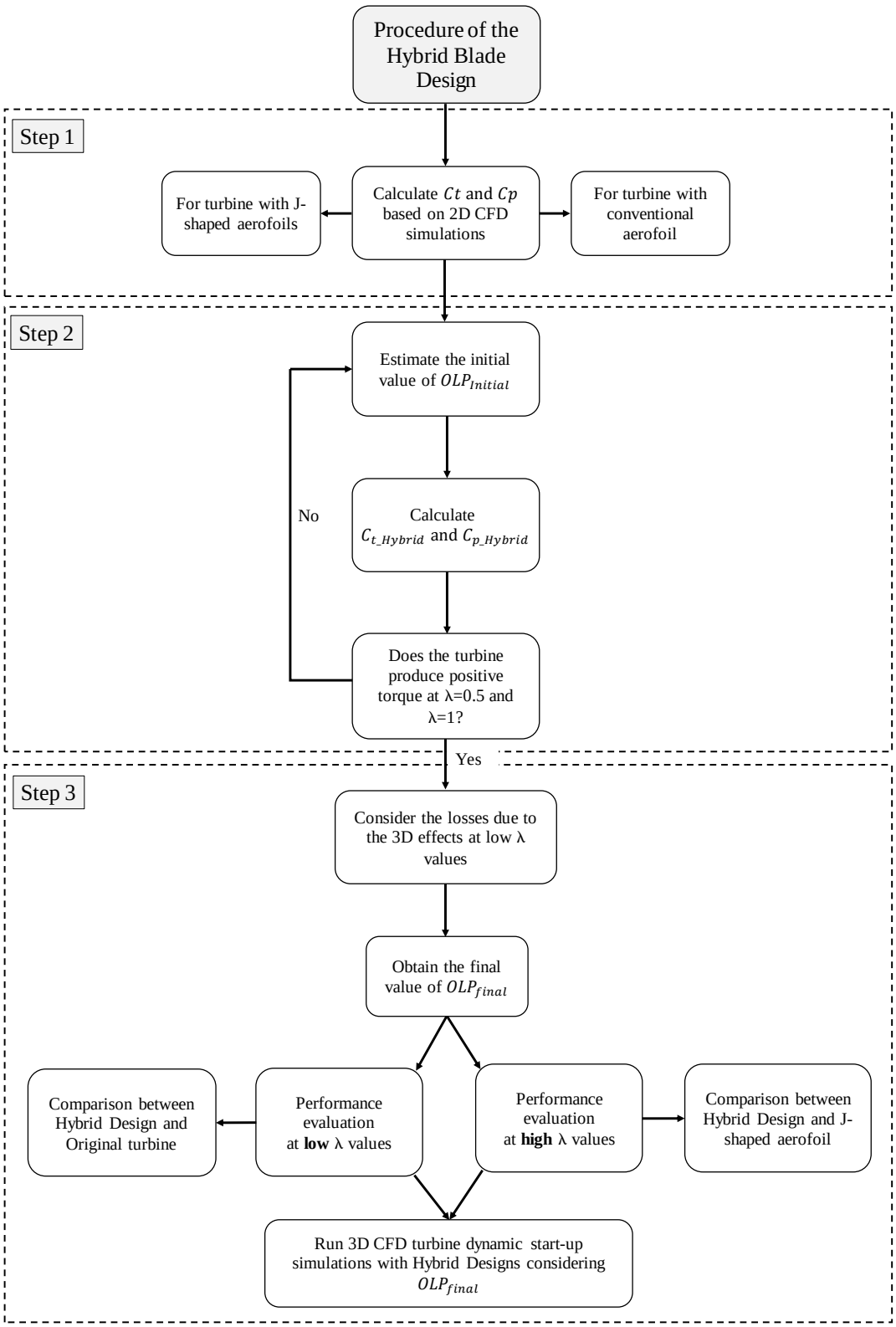

Fig. 7. Summary of the proposed hybrid blade design method (OLP: Opening Length Percentage).

Step 1: Performance analysis of the individual H-type Darrieus VAWT in 2D with the conventional airfoil and the J-shaped profiles considering the various range of the openings over the airfoil surface have been conducted (see Celik et al. (2022)). As an example, the schematic of

the airfoils with and without openings (e.g., No cutting (0%), 10% and 90%) has been demonstrated in Fig. 8.

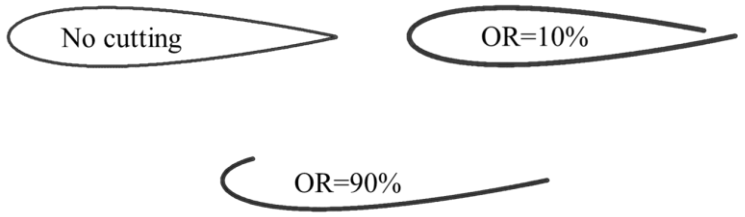

Fig. 8. The schematic of the airfoils with and without openings (OR: Opening Ratio over the J-shaped airfoil).

The torque coefficient (Ct) was calculated for the turbines investigated based on the 2D CFD calculations and the results are illustrated in Fig. 9. As illustrated in the figure, the turbines with the conventional airfoil and the J-shaped profile with a 10% opening ratio produce a negative torque at low tip speed ratios, such as λ=0.5 and λ=1, which indicates a non-self-starting capability. Furthermore, as found in the authors' previous study (Celik, 2021), when the estimated value for the resistance due to the bearing friction is implemented in the calculations, the turbine with the J-shaped profile with 20% and 30% opening ratios also do not show the self-starting capability. Therefore, in the current hybrid design study, the NACA0018 airfoil profile has been selected as a conventional airfoil, while the 40% and 90% opening ratios being selected for the J-shaped profiles. The reason behind choosing these opening ratios for the J-shaped profiles to investigate is as a result of the high computational cost required for the additional 3D CFD simulations and from the aerodynamic point of view, no significant difference is expected between the hybrid blades having the J-shaped profile with 40% and 60% openings, especially at low λ region.

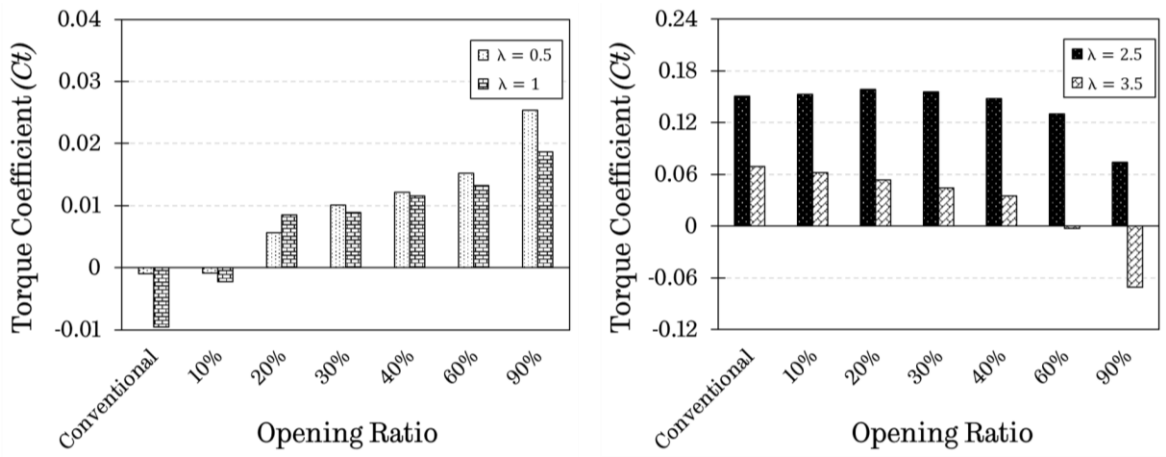

Fig. 9. Turbine torque coefficients obtained from the 2D CFD model for the airfoils investigated at different tip speed ratios.

Step 2: The most crucial part of the Step 2 is to estimate the initial opening length percentage ($OLP_{initial}$) for the J-shaped profile used in the hybrid blade design, which is related to the ratio of the length of the J-shaped profile along z direction (L_J) to the length of the whole blade span (H), (see Fig. 10).

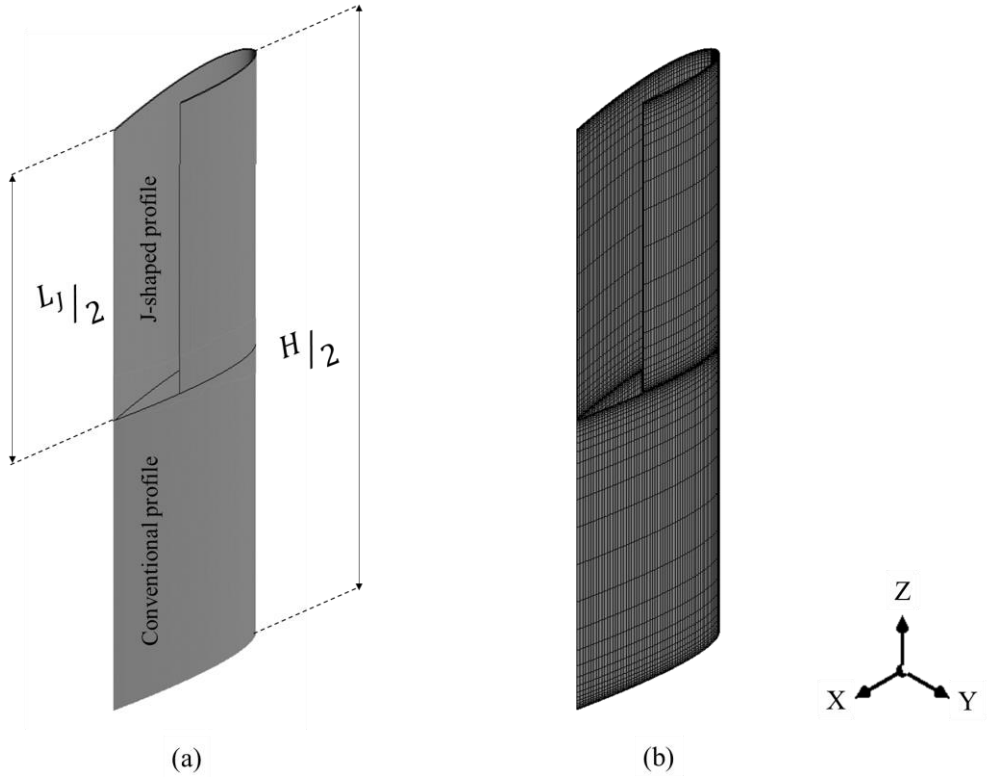

Fig. 10. (a) The demonstration of the location of the J-shaped and conventional profiles in the hybrid blade design along z direction considering half-span (b) mesh configuration of the hybrid blade.

The values estimated for the $OLP_{initial}$ are changed from 0% to 100% in order to achieve the optimum values of the OLP that provides a sufficient self-starting ability and less power loss at higher rotational speeds. Since the torque coefficient values of the turbines with the conventional airfoil ($Ct_{conventional}$) and the J-shaped profile ($Ct_{J-shaped}$) have been calculated in Step 1, the torque coefficient (Ct_{Hybrid}) of the turbine with the hybrid blade can be calculated with the estimated $OLP_{initial}$ value at the tip speed ratios investigated using the following equation:

$$Ct_{Hybrid} = Ct_{J-shaped} \times OLP + Ct_{conventional} \times (1 - OLP) \quad (1)$$

This process continues by changing the value of the $OLP_{initial}$ until the positive torque coefficient (Ct_{Hybrid}) for the turbine with a hybrid blade profile at λ=0.5 and λ=1 is obtained. For instance, the Hybrid Blade 1 design, which is the combination of the conventional airfoil and the J-shaped profile having a 40% opening, when the $OLP_{initial}$ is selected as 45% , the turbine can produce a

positive torque at the λ=0.5, but not at the λ=1; however, when $OLP_{initial}$ is selected as 46% the turbine can produce a positive torque at both λ values of 0.5 and 1. Therefore, the minimum required $OLP_{initial}$ value for the Hybrid Blade 1 to produce a positive torque coefficient at both low λ values is 46%. On the other hand, the minimum required $OLP_{initial}$ value for the turbine to obtain a positive torque generation at the λ=0.5 and λ=1 is found to be as 34% for the combination of the conventional airfoil and the J-shaped profile with a 90% opening ratio, namely the Hybrid Blade 2. Although a further increment on the $OLP_{initial}$ value would increase the turbine self-starting ability by increasing the torque generation at the low tip speed ratios, it will cause a significant performance reduction at the high tip speed ratios. Therefore, the optimum value of the $OLP_{initial}$values should also be determined by considering the turbine performance at the relatively high tip speed ratios.

Step 3: Since the estimation of the $OLP_{initial}$ values has been determined based on the 2D CFD calculations, the importance of the 3D effects has not been considered in the present performance predictions. Therefore, the values of the $OLP_{initial}$ may not be sufficient for the hybrid blades to provide the required torque to self-start the turbine. Even though the discrepancy between the 2D and 3D CFD simulations varies relying on the changes in the tip speed ratio (Franchina et al., 2019), from the literature survey, a maximum deviation has been found at around 10% in the critical region for the turbine start-up behaviour, where λ<1 (Franchina et al., 2020; Mannion et al., 2018; Orlandi et al., 2015). For this purpose, an additional factor, which is determined by considering this deviation, has been taken into account in the calculations of the final values of the percentage length of the J-shaped blade (OLP_{final}). Since the λ=1 appears to be more sensitive than the λ=0.5 in terms of the negative torque generation (see Step 2), the additional factor, which was selected as 10% in the present study, has been only added to the torque coefficient (Ct_{Hybrid}) of the hybrid bladed turbines with the $OLP_{initial}$ values at λ=1. Thus, the OLP_{final} values were estimated as 50% and 38% for the proposed Hybrid Blade 1 and Hybrid Blade 2, respectively.

As stated earlier, in the authors' previous study, a comprehensive investigation on the turbine blades having various ranges of openings, from 0% to 90%, was carried out based on the 2D-based CFD simulations considering different tip speed ratios (see Celik et al. (2022)). The results of the conventional airfoil and its J-shaped profiles with 40% and 90% openings are indicated in Fig. 11. As it is apparent in the figure, turbine having the J-shaped profiles indicates the best performance at the low λ values, while the turbine having the conventional airfoil profile produces more torque at the relatively higher λ values. However, the preliminary performance estimations of the turbine having the proposed hybrid blade designs in the present study illustrate that the

proposed designs can effectively produce much more sufficient torque compared to the turbine with a conventional airfoil at the low λ values, while there are less efficiency losses compared to the turbine with the pure J-shaped profiles at the high λ values. Therefore, the initial performance prediction obtained using the design methodology indicate that the proposed Hybrid Blades may address the disadvantages of each turbine design using a single airfoil profile and obtain the self-starting ability at low tip speed ratios and high Ct at high tip speed ratios.

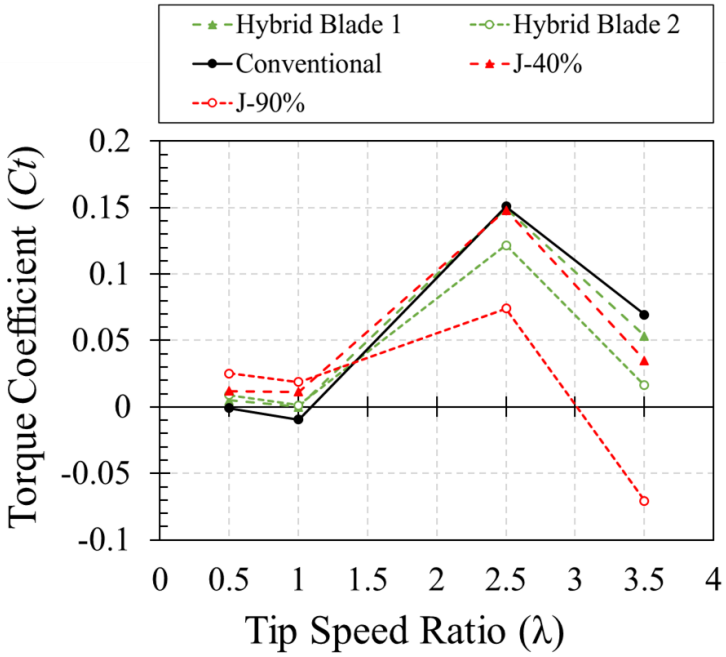

Fig. 11. Estimated torque coefficients for the turbines having different blade profiles.

In Fig. 12, the estimated torque coefficients of the proposed hybrid blade designs in a comparison with their conventional and the J-shaped profiles at different tip speed ratios are also demonstrated in order to further illustrate the advantages of the hybrid blade designs over the conventional airfoil and the J-shaped profiles considering the low and high tip λ values, respectively. The turbines with the proposed hybrid blade designs produce much higher torque coefficients compared to the turbine with the conventional airfoil at λ=0.5 and λ=1, as seen in the figure. Moreover, at relatively high tip speed ratios such as λ=2.5 and λ=3.5, the proposed designs also superior compared to the J-shaped airfoil, particularly at the highest tip speed ratio investigated. Consequently, the observed findings in this preliminary estimation process clearly demonstrate the need for the hybrid blade design used in the H-type Darrieus wind turbine to enhance the start-up ability without a large efficiency loss at the higher tip speed ratios.

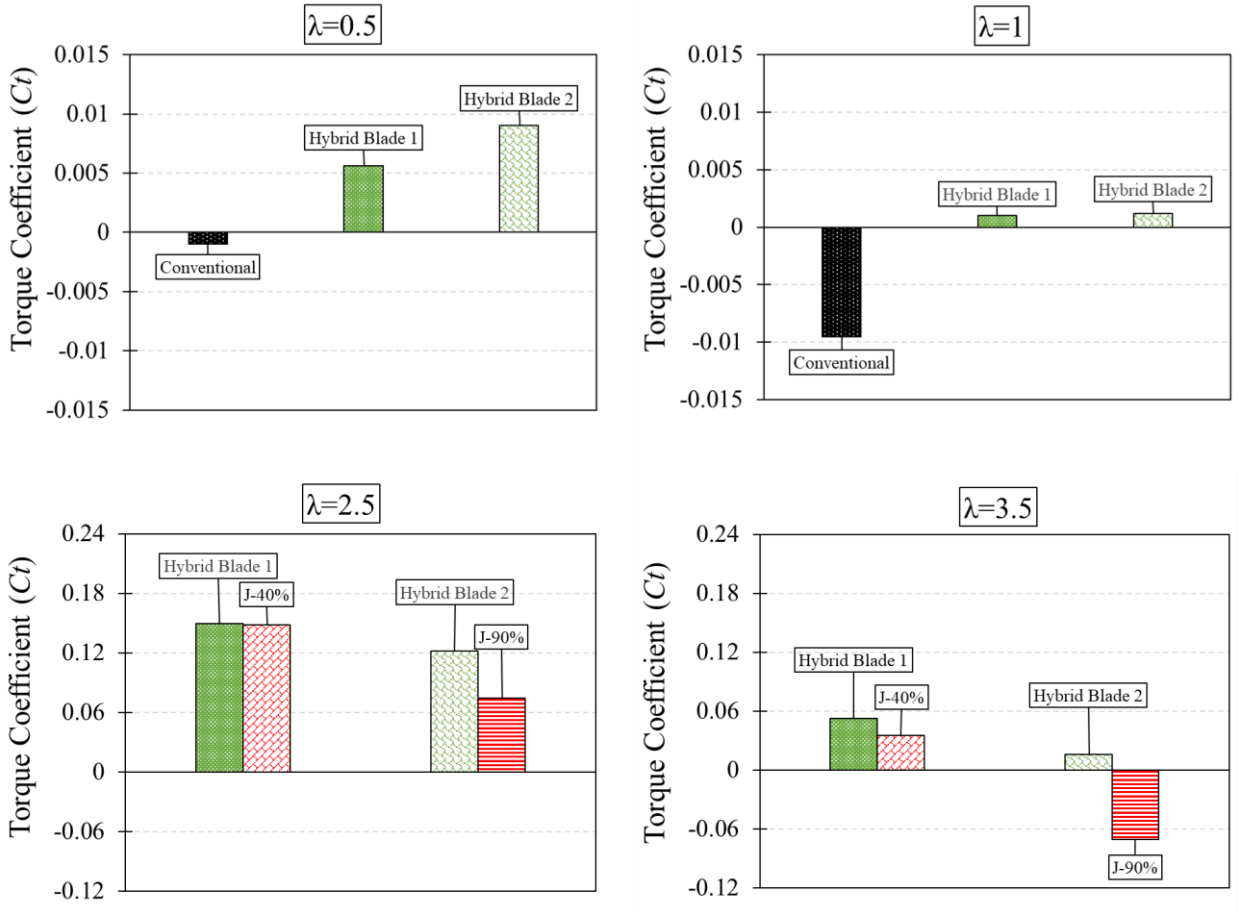

Fig. 12. Estimated torque coefficient of the hybrid blade designs in comparison with the conventional and J-shaped airfoil profiles at different tip speed ratios.

The proposed Hybrid Blade 1 and Hybrid Blade 2 are presented in Fig. 13 and Fig. 14, respectively, according to the design method explained above. Since the effect of the location of the J-shaped profile along the z direction on the aerodynamic performance of the turbine cannot be taken into consideration with the 2D-based design methodology, three different scenarios have been selected to evaluate the impact of the proposed hybrid blade design on the overall and self-starting performance of the H-type Darrieus VAWTs for the current 3D CFD investigations. The three scenarios are (a) the J-shaped being placed at the top and the bottom of the blade with an open tip end, (b) the J-shaped being placed at the top and the bottom of the blade with a closed tip, and (c) the J-shaped being placed at the middle of the blade span.

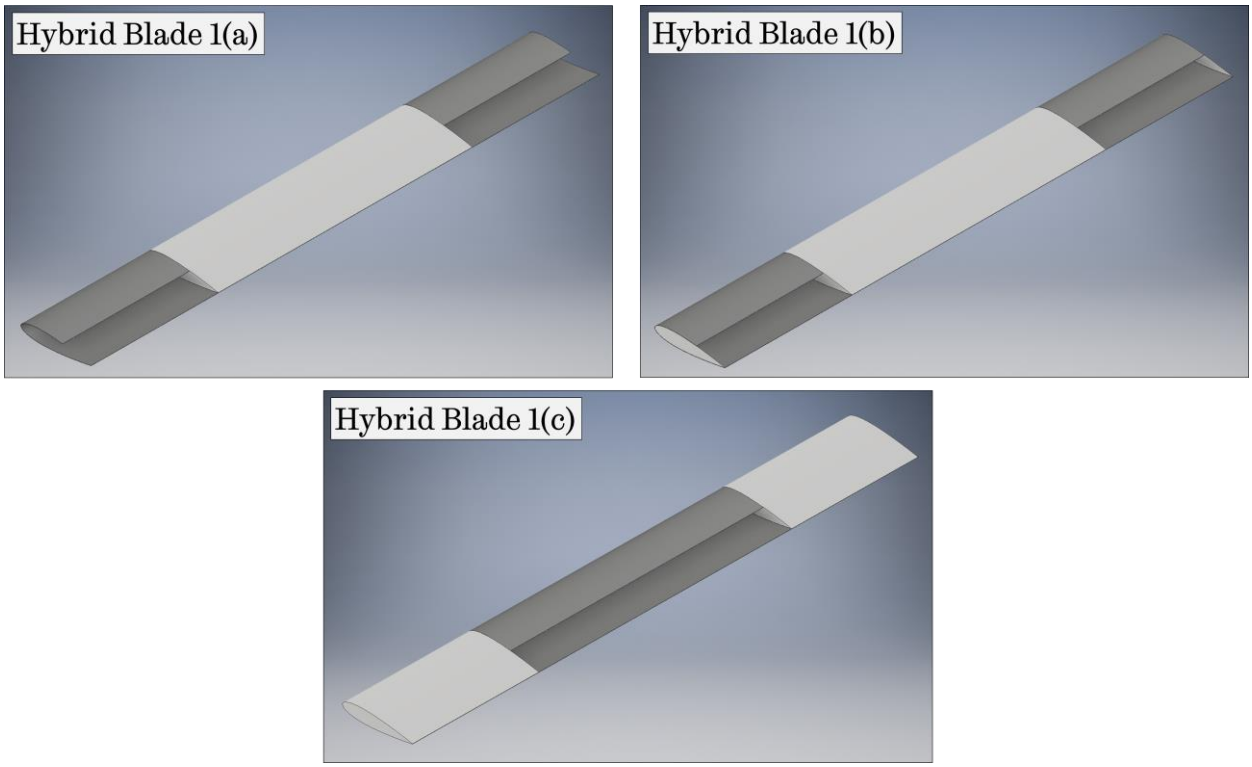

Fig. 13. Schematic for the different configurations of the proposed Hybrid Design 1.

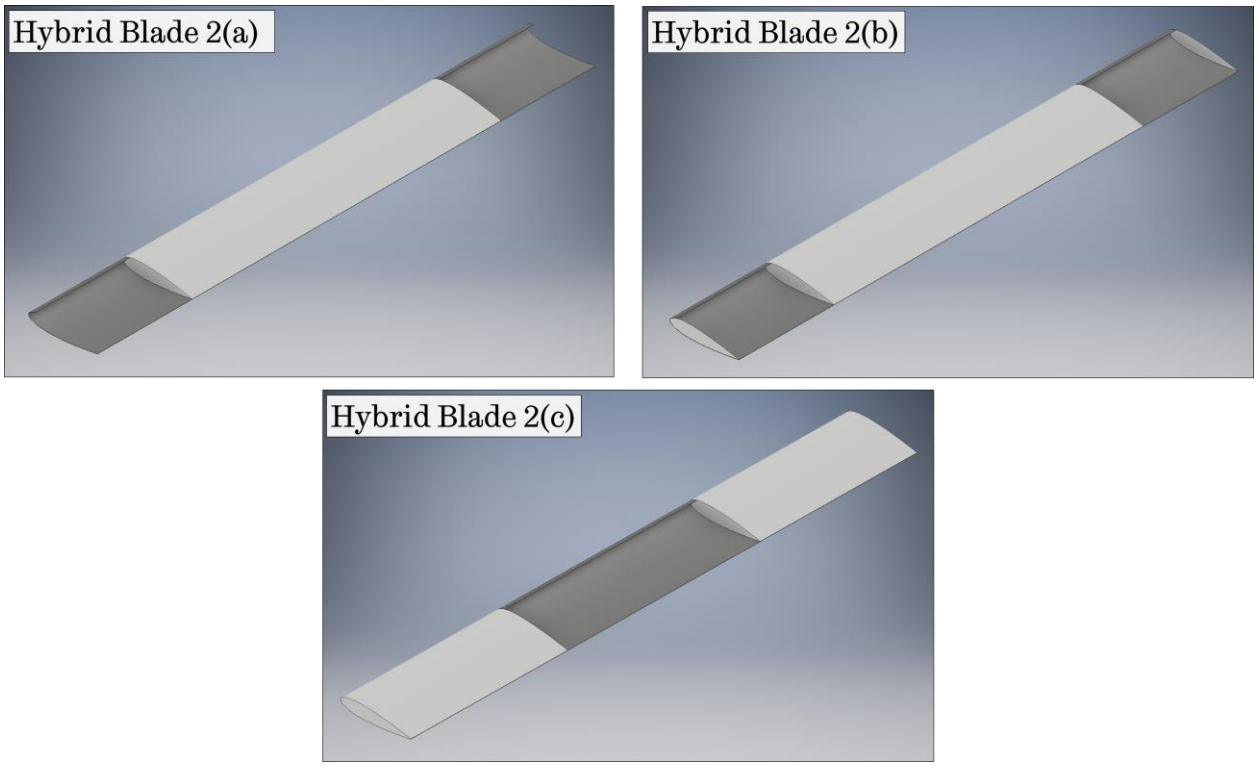

Fig.14. Schematic for the different configurations of the proposed Hybrid Design 2.

4. Results and discussions

The objective of the present section is to investigate the effect of the proposed hybrid blade configurations, namely Hybrid Blade 1 (a,b, and c) and Hybrid Blade 2 (a,b, and c), on the overall performance and the self-starting characteristics of the Darrieus type wind turbine with the aid of the 3D CFD start-up modelling. For the current investigations, the turbine with a radius of 0.375m, the blade chord length of 0.083m, and the height of 0.6m has been employed under the free wind speed of 5 m/s.

Fig. 15 demonstrates the impact of the different hybrid blade configurations on the dynamic start-up behaviour of the turbine in comparison with their conventional blade profile and pure J-shaped airfoils, such as the 40% and 90% opening J-shaped profiles. The results show that the turbine with the conventional airfoil, which is the NACA0018 in the present study, does not illustrate the self-starting characteristics. On the other hand, although the 40% opening J-shaped airfoils having open and closed tips show a superior start-up ability compared to the proposed hybrid blades from the start-up time point of view, a remarkable decrease in the maximum tip speed ratio has been observed when the steady-state condition was achieved. Moreover, it can be clearly observed in Fig. 15 that the turbines with the J-shaped profiles placed at the top and bottom of the blade with a closed tip exhibit a higher final tip speed ratio, which results in a wider turbine operating range, and the start-up time required to reach the steady-state condition compared to their open tip configuration in both proposed designs. Moreover, no significant difference has been observed between the hybrid blade configurations b and c in both the Hybrid Blade designs. The results clearly illustrate that even though the location of the J-shaped profile does not have much impact on the turbine self-starting characteristics, a significant discrepancy in the self-starting behaviour of the turbine can be observed when closed and open tip is used at the blade tip. It is believed that the reason behind this situation is that the tip vortex generated at the blade tip, which causes a different vortex structure and changes the severity of the pressure interactions between the two sides of the blade. Therefore, a more detailed illustration will be provided using the contours of both pressure coefficient and vorticity for the comparison of the effect of the shape of the tip on the performance of the turbine in the following sections.

The summary of the findings obtained from the present analyses is shown in Table 2. The table clearly illustrates that the turbine with the Hybrid Blade 1(b) configuration has the maximum final tip speed ratio with a value of 3.35, and therefore its self-starting performance is the best among all the six configurations investigated. On the other hand, the amount of time needed for the

turbines to reach the steady-state conditions increases with the turbines having the Hybrid Blade 1(a) and Hybrid Blade 2(a) with a much lower final λ.

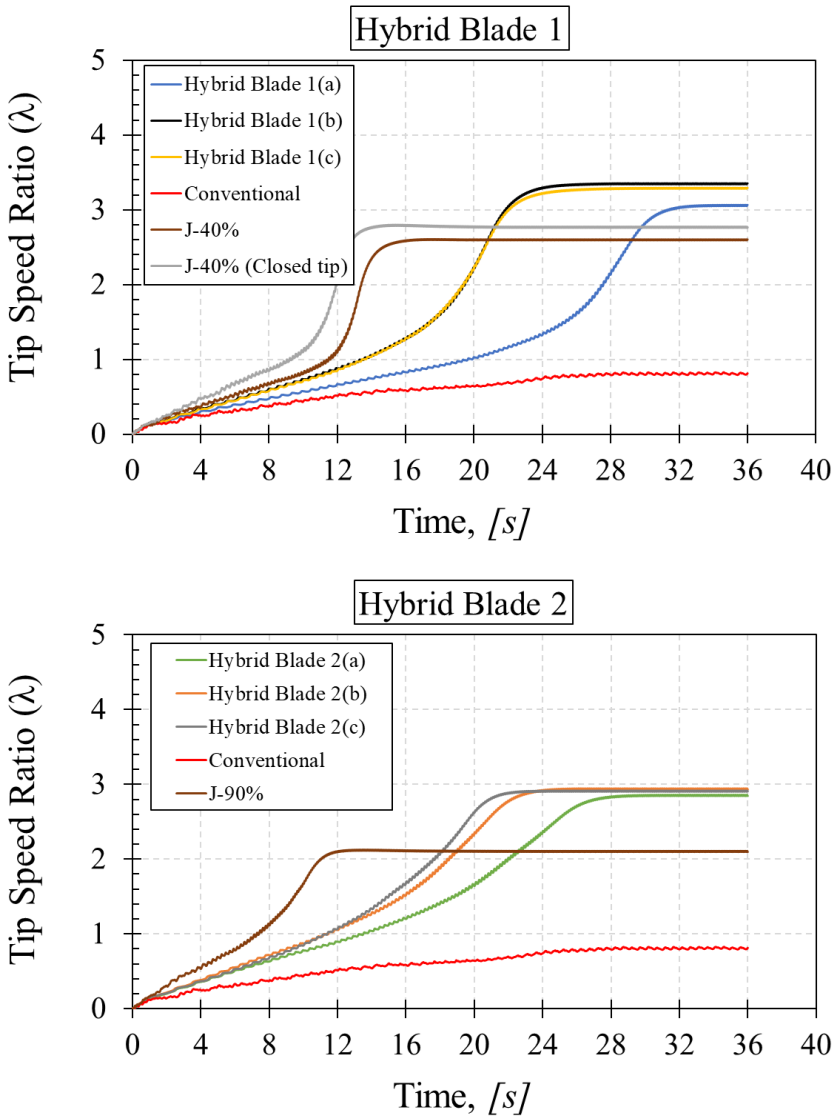

Fig. 15. The comparison of the start-up process of different hybrid blade configurations.

Table 2. The comparison of the start-up performance of the proposed hybrid blade designs investigated with the conventional and pure J-shaped profiles.

	Conventional	J-40%	J-90%	Hybrid Blade 1			Hybrid Blade 2		
				a	b	c	a	b	c
Self-starting capability	No	Yes	Yes	Yes	Yes	Yes	Yes	Yes	Yes
Self-starting time (s)	—	17.4	13.6	34.2	26.8	26.9	30.4	26.2	24.1
Final λ	—	2.6	2.1	3.07	3.35	3.29	2.85	2.93	2.9

In order to discuss the effect of the different hybrid blade configurations on the aerodynamic performance of the H-type Darrieus wind turbine, the variation of the torque coefficients and power coefficients with the tip speed ratio during the dynamic start-up process for the Hybrid Blade 1(a), 1(b), and 2(b) are plotted in Fig. 16 and Fig. 17. The comparison between the Hybrid Blade 1(a) and 1(b) will provide a further better understanding of the effect of the closed and open tip on the aerodynamic performance in the complete operating conditions. On the other hand, the comparison between Hybrid Blade 1(b) and 2(b) illustrates the effect of the usage of the different J-shaped profiles in the hybrid blade designs on the turbine overall performance.

As it is illustrated in Fig. 16, the turbine with the Hybrid Blade 1(b) has the best performance in the entire turbine operating range compared to the Hybrid Blade 1(a). Therefore, this result supports the findings from the dynamic start-up characteristics. For example, the generation of the higher torque coefficient at low and high tip speed ratio results in a faster start-up and a higher final rotational speed at the steady-state condition, respectively. On the other hand, when we compare the performance of the Hybrid Blade 1(b) and Hybrid Blade 2(b), it can be seen in Fig. 17 that Hybrid Blade 2(b) has the higher performance in the low λ region ($0<\lambda<1.5$). However, the highest performance at the relatively high λ region ($1.5<\lambda<3.35$) can be achieved with the Hybrid Blade 1(b). This leads to a faster turbine acceleration with the Hybrid Blade 2(b) and a higher final tip speed ratio at the steady-state condition with the Hybrid Blade 1(b) (see Fig. 15).

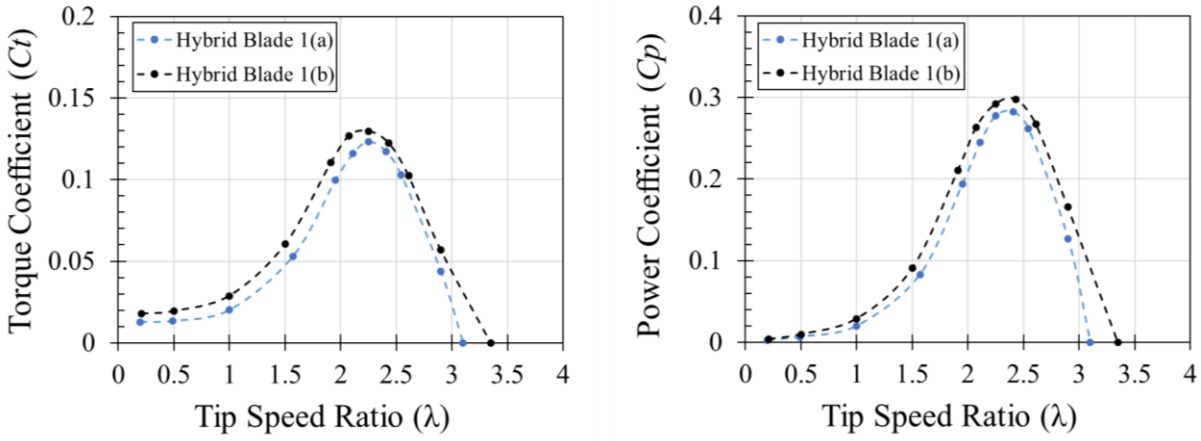

Fig. 16. The comparison of the torque and power coefficients of the turbines with the Hybrid Blade 1(a) and Hybrid Blade 1(b) at various tip speed ratios.

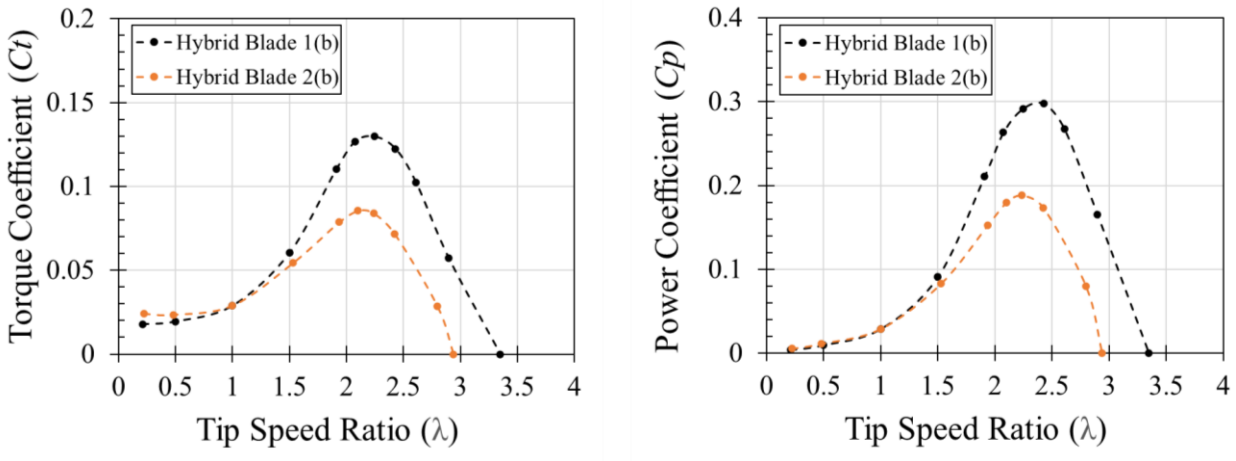

Fig. 17. The comparison of the torque and power coefficients of the turbines with the Hybrid Blade 1(b) and Hybrid Blade 2(b) at various tip speed ratios.

As mentioned before, although the same configuration, except the closed or open tip, is used in the Hybrid Blade 1(a) and Hybrid Blade 1(b), the difference on the overall performance between the turbines with these configurations is apparent. This may be due to the effect of the tip vortex generated at the blade tips. However, the aerodynamic performance difference between the Hybrid Blade 1(b) and Hybrid Blade 2(b) is considered to be the utilisation for the different J-shaped profile in these configurations. For instance, a 40% opening is used for the Hybrid Blade 1(b) while a 90% opening is used in Hybrid Blade 2(b). To better analyse and explain the difference between these configurations, the variation of the instantaneous blade torque coefficient over a complete blade revolution at different tip speed ratios is illustrated in Fig. 18. This figure shows that a slightly higher torque coefficient can be obtained in the upwind part of the turbine with the Hybrid Blade 2(b) configuration while the torque pattern of these three configurations is similar at the low tip speed ratios, for instance λ=0.5 and λ=1. This results in a higher torque coefficient generation at these two tip speed ratios (see Fig. 17). The plausible explanation for this situation may be due to the fact that the usage of a J-shaped profile with the larger opening ratio, such as 90%, increases the torque generation in the upwind part of the turbine, especially at the low λ values, while it decreases the torque generation in the downwind part of the turbine, especially at the relatively higher λ values.

Furthermore, at the relatively higher tip speed ratios, such as λ=2.25 and λ=2.9, a much more obvious difference in the torque generation can be observed between the different hybrid blade configurations compared to the low λ values. Although the Hybrid Blade 1(b) and Hybrid Blade 2(b) have a similar torque generation in the upwind part of the turbine ($0° < \theta < 180°$), the

Hybrid Blade 1(b) performs the best in the downwind part of the turbine ($180° < \theta < 360°$). This difference may be because of the utilisation of a 40% opening, which has a lower performance loss in the downwind part of the turbine, in the Hybrid Blade 1(b), while a 90% opening, which has relatively higher performance loss, in the Hybrid Blade 2(b). Furthermore, when the Hybrid Blade 1(b) is compared to the Hybrid Blade 1(a), the difference in the torque generation, in particular in the upwind part of the turbine, may be because of the blade tip effect.

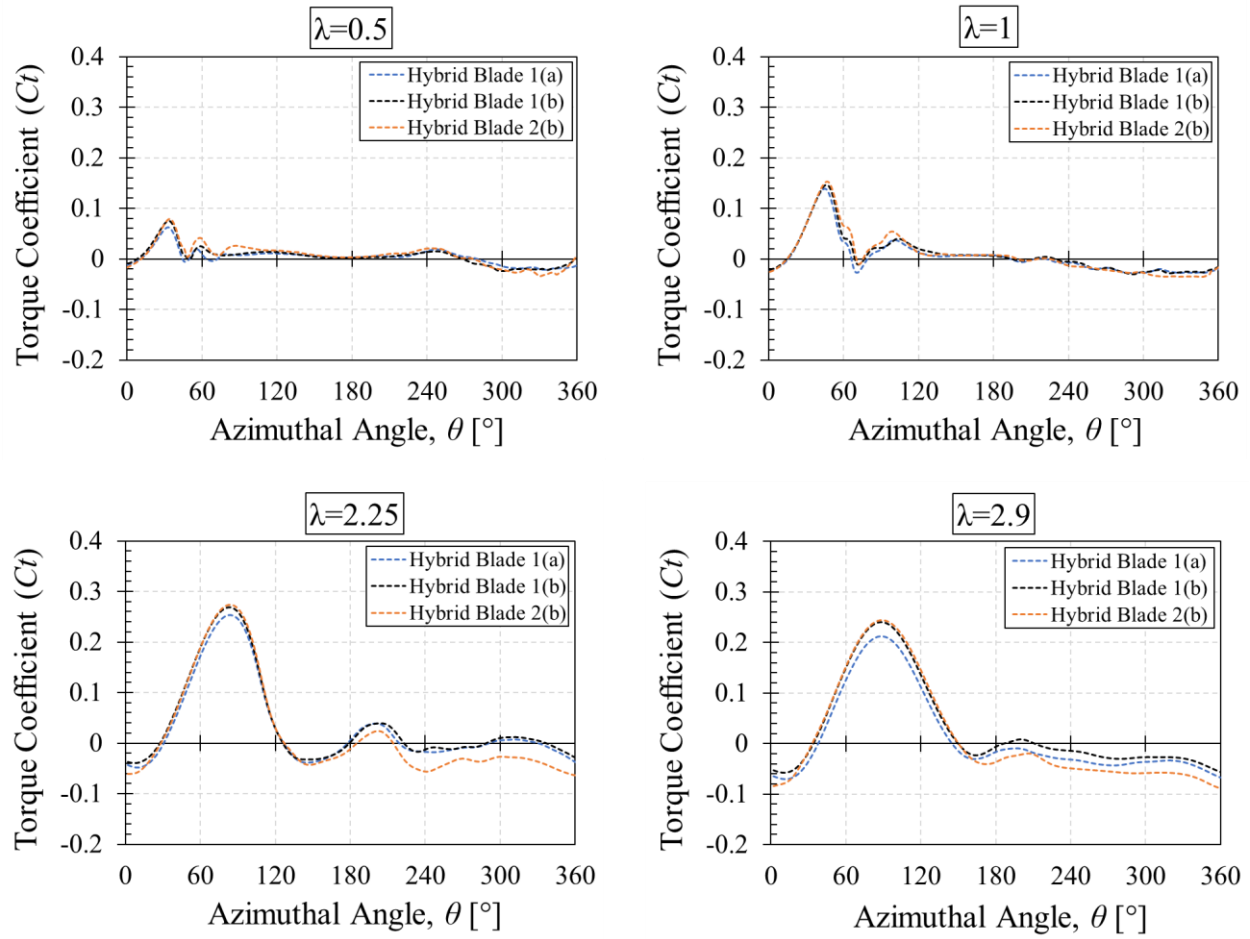

Fig. 18. Variations of the blade torque coefficients with the azimuthal angle for the turbines having Hybrid Blade 1(a), Hybrid Blade 1(b), and Hybrid Blade 2(b) at various tip speed ratios.

Furthermore, the lift and drag coefficient of the three configurations at the optimum λ of 2.25 are illustrated in Fig. 19. It should also be noted that for simplification purposes, the theoretical angle attack has been used in the calculations. As can be seen from this figure, although no considerable difference in the lift coefficient is observed between the hybrid blade configurations in the positive angles of attack region, which is corresponding to the upwind part of the turbine, the Hybrid Blade 1(a) produces a much higher drag coefficient in the upwind part of the turbine, which results in a much lower performance at the values of λ investigated (see Fig. 18). On the other hand, a lower torque coefficient in the downwind part of the turbine is obtained with the Hybrid Blade 2(b) at

λ=2.25 as illustrated in Fig. 18. The reason for this is the generation of the higher drag coefficient in the negative angles of attack region, which is corresponding to the downwind part of the rotor, because of the utilisation of a 90% opening.

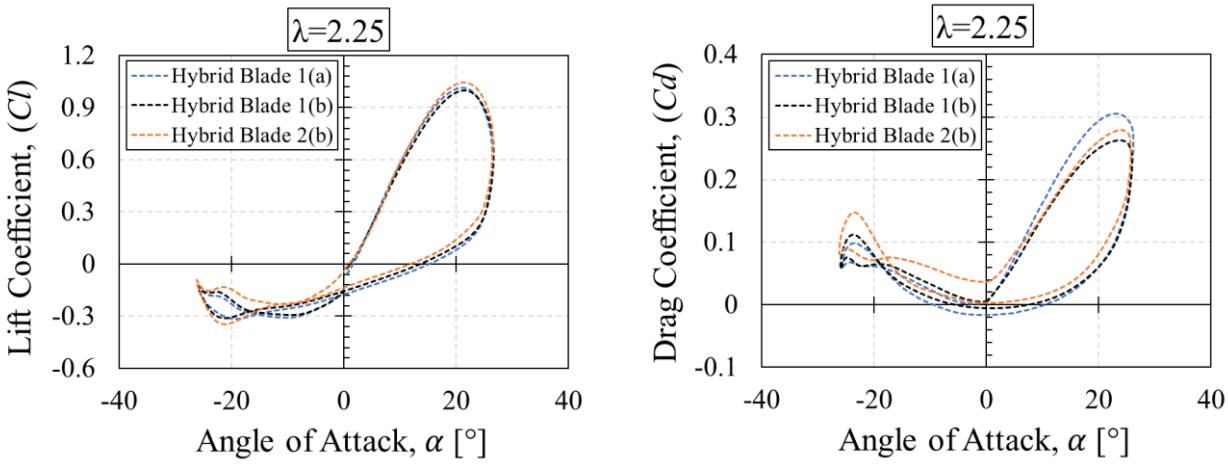

Fig. 19. Comparison of the lift coefficient and drag coefficient between the hybrid blade designs investigated at tip speed ratio of 2.25.

The pressure coefficient distributions on both the pressure and suction sides of the proposed Hybrid Blade 1(a) and Hybrid Blade 1(b) at the tip speed ratio of 2.25 have been illustrated in Fig. 20 considering different locations along the spanwise direction at $\theta = 90°$. As it can be observed in the figure that in the blade sections where the conventional airfoils located (y3 and y4), the pressure distribution over the pressure and suctions sides of both the proposed hybrid blades shows a similar behaviour. However, when the blade sections where the J-shaped airfoils located (y1 and y2) are considered, the pressure difference between the sides are increased throughout the blade tips. A higher pressure difference at the blade tip of the Hybrid Blade 1(b), which has a closed tip, has been obtained compared to the Hybrid Blade 1(a), which has an open tip. This situation results in a higher torque coefficient generation at the tip speed ratio investigated when a proposed hybrid blade that has a closed tip is employed in the turbine (see Fig. 16).

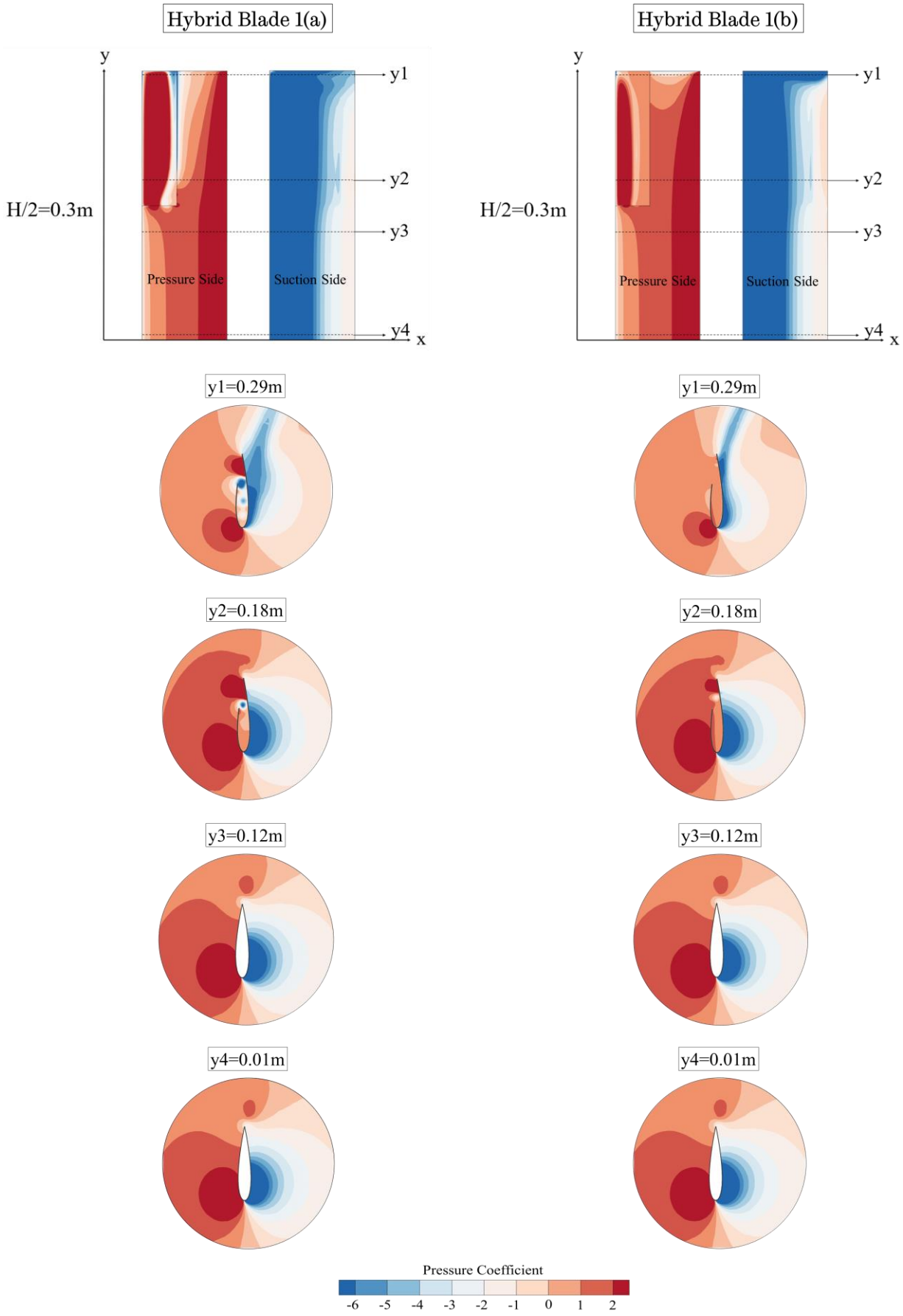

Fig. 20. Comparison of the pressure coefficient distribution on the blade pressure and suction sides of Hybrid Blade 1(a) and Hybrid Blade 1(b) at different locations along the spanwise direction at λ=2.25.

For further analyses on the difference between the Hybrid Blade 1(a) and Hybrid Blade 1(b), the vortex structure over the blades with the open and closed tips at the same turbine positions are shown by the iso-surface of Q=0.005 coloured by the velocity magnitude in Fig. 21 and Fig. 22 considering the optimum λ of 2.25. The comparison of the iso-surface contours between these two configurations provides a more in-depth understanding of the effect of the closed and open tips on the hybrid blade performance. The utilisation of the closed tip can affect the distribution of the vorticities over the blade tip. As can be observed from the figures, a larger vortex structure has been generated with the hybrid blade with an open tip (Hybrid Blade 1(a)) compared to the closed tip (Hybrid Blade 1(b)). Since a larger vortex structure at the blade tip indicates a more intense pressure interaction between the pressure and the suction sides, this leads to a reduction in the pressure difference between two sides of the blade and as a result a decrease in the power efficiency. On the contrary, when we consider the Hybrid Blade 1(b), a reduced tip vortex structure can be observed and it can visually demonstrate a much weaker pressure interaction between the pressure and suction sides at the closed tip and an improvement in the turbine performance. Moreover, in the case of the Hybrid Blade 1(a), it appears that air finds its own way to escape from the blade tips, which may result in a lower pressure difference between the inner and outer sides of the J-shaped profile used in the Hybrid Blade 1(a) and lower performance compared to the Hybrid Blade 1(b).

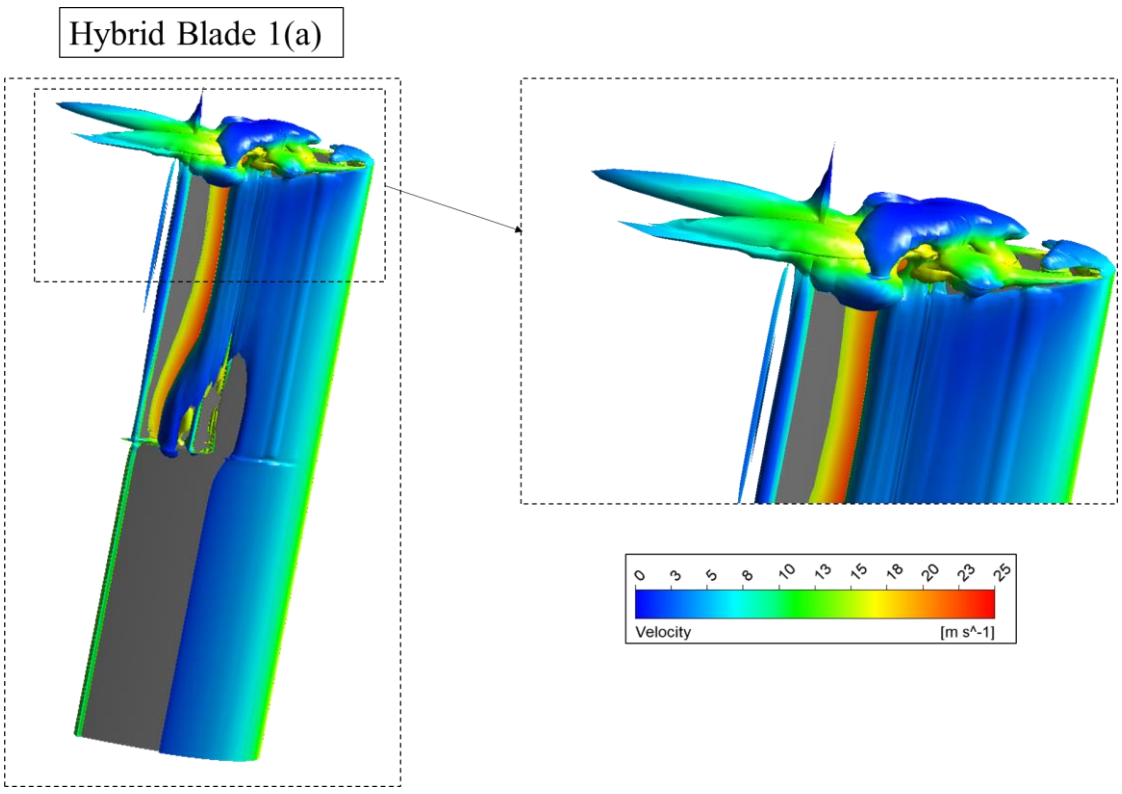

Fig. 21. The iso-surface contours for the vortex structures generated around the turbine with the Hybrid Blade 1(a) configuration with an enlarged view of the blade tip at λ=2.25.

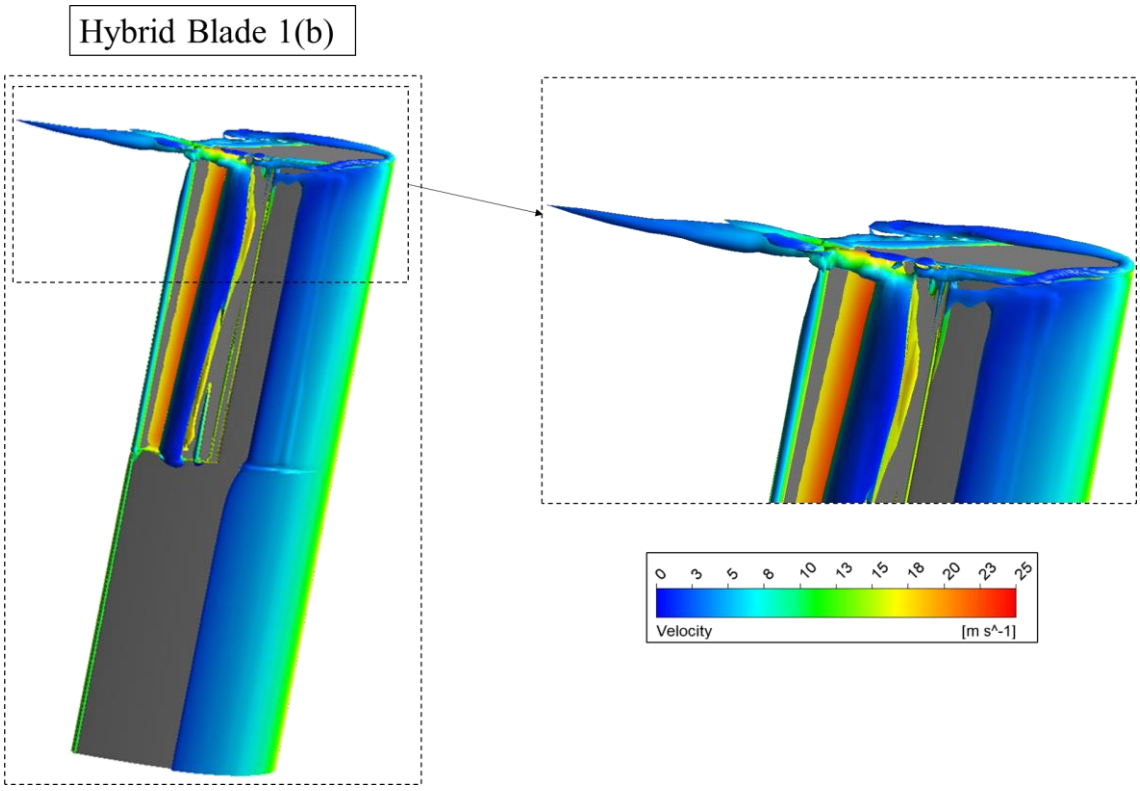

Fig. 12. The iso-surface contours for the vortex structures generated around the turbine with the Hybrid Blade 1(b) configuration with an enlarged view of the blade tip at λ=2.25.

5. Conclusion

In this study, for the first time, a novel hybrid blade design has been proposed to overcome the low torque generation capability of the conventional airfoil at low λ values and higher torque losses of the pure J-shaped profiles at the higher λ values. For this purpose, a new design methodology based on the 2D CFD calculations has been proposed in order to accurately predict the torque and power generations of the turbine with the hybrid blades at different turbine operating conditions. Then, due to the inherent shape of the proposed hybrid blade designs, a 3D-based CFD start-up modelling strategy and validation study for the model in comparison with the 2D-based CFD start-up model and the experimental study have been conducted. Finally, a new computationally affordable 3D CFD model has been employed for the analyses of the proposed hybrid blade designs from the overall performance and self-starting behaviour point of view.

The following conclusions can be drawn based on the findings obtained in the current study:

- The proposed 2D-based design methodology provides the first insight into the performance of the hybrid blade designs and consistent results were obtained between the 3D CFD simulations and the proposed design methodology.

- Considering the maximum tip speed ratio value at the steady-state conditions and the start-up time, Hybrid Blade 1(b), which has a closed-tip, demonstrates a better aerodynamic performance compared to the Hybrid Blade 1(a), which has an open-tip.
- It has been found that in contrast to the J-shaped airfoil with open or closed-tips, the location of the J-shaped airfoil in the hybrid blade span does not considerably influence the turbine start-up capability.
- Even though the Hybrid Blade 1(b) and Hybrid Blade 2(b) can show the similar instantaneous torque generation in the upwind part of the turbine at the tip speed ratios studied, Hybrid Blade 2(b) illustrates a less torque generation in the downwind part of the turbine, especially at the relatively higher λ values. This may be due to the utilisation of the J-shaped airfoil with a larger opening (e.g. 90%), which provides a considerably higher negative drag contribution.
- Among all the designs investigated, the turbine with the Hybrid Blade 1(b), which consists of the conventional airfoil NACA0018 and its closed-tip J-shaped profile with a 40% opening ratio, demonstrates a better overall and the self-starting performance.

The limitation of the present study and recommended future work:

- The 2D-based CFD model has been used due to its simplicity for the torque coefficient prediction of the hybrid blade designs. However, a full 3D CFD model is recommended for the performance predictions during the design methodology process.
- It is recommended to conduct further studies on the hybrid blade design to provide an in-depth understanding of the different design configurations and solid conclusions about the blade behaviour.
- It would be beneficial to conduct a study that investigates the effect of the different types of tips of the 3D hybrid blade design, such as winglet, on the self-starting performance.
- Apart from the aerodynamic performance comparison between the Hybrid blade and the Hybrid turbine, a further study on the techno-economic analysis and Life Cycle analysis is recommended in order to indicate the advantages of the Hybrid blade over the Hybrid turbine.
- Conducting an experimental investigation would be helpful to provide a further understanding of the impact of the hybrid blade design on the turbine's overall and start-up performance.
- Since a relatively thin sheet material used for the J-shaped profile, it might lead to a much lower mechanical resistance compared to the conventional profile. Therefore, an investigation on the types and the thickness of the material would be an interesting research topic by considering variation and high-strength design method of the H-type VAWT having a J-shaped airfoil.

Acknowledgment

Yunus Celik would like to express his gratitude to the Ministry of National Education (Turkey) for funding his Ph.D. studies.

Appendix

The User-Defined Function code including the physical properties of the turbine was used in the present 3D CFD simulations in order to calculate the rotational speed of the turbine. It is also important to note that the moment of inertia of the turbine was recalculated considering the per unit span.

```
#include "udf.h"

DEFINE_SDOF_PROPERTIES(rotor, prop, dt, time, dtime)
{
  prop[SDOF_MASS]         = 0.064;
  prop[SDOF_IXX]          = 0.009;
  prop[SDOF_IYY]          = 0.009;
  prop[SDOF_IZZ]          = 0.009;

  prop[SDOF_ZERO_TRANS_X] = TRUE;
  prop[SDOF_ZERO_TRANS_Y] = TRUE;
  prop[SDOF_ZERO_TRANS_Z] = TRUE;

  prop[SDOF_ZERO_ROT_X] = TRUE;
  prop[SDOF_ZERO_ROT_Y] = TRUE;
  prop[SDOF_ZERO_ROT_Z] = FALSE;

  printf ("\n Blade updated 6DOF properties");
}
```

References

Abdalrahman, G., Daoud, M.A., Melek, W.W., Lien, F.S., Yee, E., 2022. Design and Implementation of an Intelligent Blade Pitch Control System and Stability Analysis for a Small Darrieus Vertical-Axis Wind Turbine. Energies 15. https://doi.org/10.3390/en15010235

Abdolahifar, A., Karimian, S.M.H., 2022. A comprehensive three-dimensional study on Darrieus vertical axis wind turbine with slotted blade to reduce flow separation. Energy 248, 123632. https://doi.org/10.1016/j.energy.2022.123632

Almohammadi, K.M., Ingham, D.B., Ma, L., Pourkashanian, M., 2015. Modeling dynamic stall of a straight blade vertical axis wind turbine. J. Fluids Struct. 57, 144–158. https://doi.org/10.1016/j.jfluidstructs.2015.06.003

ANSYS, 2013. ANSYS Fluent User's Guide Release 15.0. Canonsburg: ANSYS Inc.

ANSYS Inc., 2014. Introduction to Ansys Fluent-Turbulence Modeling.

Asadi, M., Hassanzadeh, R., 2022. On the application of semicircular and Bach-type blades in

the internal Savonius rotor of a hybrid wind turbine system. J. Wind Eng. Ind. Aerodyn. 221, 104903. https://doi.org/10.1016/j.jweia.2022.104903

Balduzzi, F., Bianchini, A., Maleci, R., Ferrara, G., Ferrari, L., 2016. Critical issues in the CFD simulation of Darrieus wind turbines. Renew. Energy 85, 419–435. https://doi.org/10.1016/j.renene.2015.06.048

Bhuyan, S., Biswas, A., 2014. Investigations on self-starting and performance characteristics of simple H and hybrid H-Savonius vertical axis wind rotors. Energy Convers. Manag. 87, 859–867. https://doi.org/10.1016/j.enconman.2014.07.056

Bianchini, A., Balduzzi, F., Rainbird, J.M., Peiró, J., Graham, J.M.R., Ferrara, G., Ferrari, L., 2015. On the influence of virtual camber effect on airfoil polars for use in simulations of Darrieus wind turbines. Energy Convers. Manag. 106, 373–384. https://doi.org/10.1016/j.enconman.2015.09.053

Celik, Y., 2021. Aerodynamics and Self-Starting of Vertical Axis Wind Turbines with J-Shaped Aerofoils. Univ. Sheffield, PhD Thesis.

Celik, Y., Ingham, D., Ma, L., Pourkashanian, M., 2022. Design and aerodynamic performance analyses of the self-starting H-type VAWT having J-shaped aerofoils considering various design parameters using CFD. Energy 123881. https://doi.org/doi.org/10.1016/j.energy.2022.123881

Celik, Y., Ma, L., Ingham, D., Pourkashanian, M., 2020. Aerodynamic investigation of the start-up process of H-type vertical axis wind turbines using CFD. J. Wind Eng. Ind. Aerodyn. 204. https://doi.org/10.1016/j.jweia.2020.104252

Dabiri, J.O., 2011. Potential order-of-magnitude enhancement of wind farm power density via counter-rotating vertical-axis wind turbine arrays. J. Renew. Sustain. Energy 3. https://doi.org/10.1063/1.3608170

Didane, D.H., Rosly, N., Zulkafli, M.F., Shamsudin, S.S., 2019. Numerical investigation of a novel contra-rotating vertical axis wind turbine. Sustain. Energy Technol. Assessments 31, 43–53. https://doi.org/10.1016/j.seta.2018.11.006

Dominy, R.G., Lunt, P., Bickerdyke, A., Dominy, J., 2007. Self-starting capability of a Darrieus turbine. Proc. Inst. Mech. Eng. Part A J. Power Energy 221, 111–120. https://doi.org/10.1243/09576509JPE340

Franchina, N., Kouaissah, O., Persico, G., Savini, M., 2019. Three-dimensional CFD simulation and experimental assessment of the performance of a h-shape vertical-axis wind turbine at design and off-design conditions. Int. J. Turbomachinery, Propuls. Power 4. https://doi.org/10.3390/ijtpp4030030

Franchina, N., Persico, G., Savini, M., 2020. Three-dimensional unsteady aerodynamics of a H-shaped vertical axis wind turbine over the full operating range. J. Wind Eng. Ind. Aerodyn. 206, 104273. https://doi.org/10.1016/j.jweia.2020.104273

Gao, Q., Lian, S., Yan, H., 2022. Aerodynamic Performance Analysis of Adaptive Drag-Lift Hybrid Type Vertical Axis Wind Turbine. Energies 15. https://doi.org/10.3390/en15155600

Gavaldà, J., Massons, J., Díaz, F., 1990. Experimental study on a self-adapting Darrieus-Savonius wind machine. Sol. Wind Technol. 7, 457–461. https://doi.org/10.1016/0741-983X(90)90030-6

Gupta, R., Biswas, A., 2011. CFD analysis of flow physics and aerodynamic performance of a combined three-bucket Savonius and three-bladed darrieus turbine. Int. J. Green Energy 8, 209–233. https://doi.org/10.1080/15435075.2010.548541

Hand, B., Cashman, A., 2020. A review on the historical development of the lift-type vertical axis wind turbine: From onshore to offshore floating application. Sustain. Energy Technol. Assessments 38. https://doi.org/10.1016/j.seta.2020.100646

Hosseini, A., Goudarzi, N., 2019. Design and CFD study of a hybrid vertical-axis wind turbine by employing a combined Bach-type and H-Darrieus rotor systems. Energy Convers. Manag. 189, 49–59. https://doi.org/10.1016/j.enconman.2019.03.068

Kaya, M.N., Kök, A.R., Kurt, H., 2021. Comparison of aerodynamic performances of various airfoils from different airfoil families using CFD. Wind Struct. An Int. J. 32, 239–248. https://doi.org/10.12989/was.2021.32.3.239

Khalid, M.S.U., Wood, D., Hemmati, A., 2022. Self-Starting Characteristics and Flow-Induced Rotation of Single- and Dual-Stage Vertical-Axis Wind Turbines. Energies 15, 1–19.

Liang, X., Fu, S., Ou, B., Wu, C., Chao, C.Y.H., Pi, K., 2017. A computational study of the effects of the radius ratio and attachment angle on the performance of a Darrieus-Savonius combined wind turbine. Renew. Energy 113, 329–334. https://doi.org/10.1016/j.renene.2017.04.071

Mannion, B., Leen, S.B., Nash, S., 2018. A two and three-dimensional CFD investigation into performance prediction and wake characterisation of a vertical axis turbine. J. Renew. Sustain. Energy 10. https://doi.org/10.1063/1.5017827

Mazarbhuiya, H.M.S.M., Biswas, A., Sharma, K.K., 2020. Blade thickness effect on the aerodynamic performance of an asymmetric NACA six series blade vertical axis wind turbine in low wind speed. Int. J. Green Energy 17, 171–179. https://doi.org/10.1080/15435075.2020.1712214

McLean, D., Pope, K., Duan, X., 2022. Start-up considerations for a small vertical-axis wind turbine for direct wind-to-heat applications. Energy Convers. Manag. 261, 115595. https://doi.org/10.1016/j.enconman.2022.115595

Mitchell, S., Ogbonna, I., Volkov, K., 2021. Improvement of self-starting capabilities of vertical axis wind turbines with new design of turbine blades. Sustain. 13, 1–24. https://doi.org/10.3390/su13073854

Mohamed, M.H., 2019. Criticism study of J-Shaped darrieus wind turbine: Performance evaluation and noise generation assessment. Energy 177, 367–385. https://doi.org/10.1016/j.energy.2019.04.102

Mohamed, O.S., Elbaz, A.M.R., Bianchini, A., 2021. A better insight on physics involved in the self-starting of a straight-blade Darrieus wind turbine by means of two-dimensional Computational Fluid Dynamics. J. Wind Eng. Ind. Aerodyn. 218, 104793. https://doi.org/10.1016/j.jweia.2021.104793

Naseem, A., Uddin, E., Ali, Z., Aslam, J., Shah, S.R., Sajid, M., Zaidi, A.A., Javed, A., Younis, M.Y., 2020. Effect of vortices on power output of vertical axis wind turbine (VAWT). Sustain. Energy Technol. Assessments 37, 100586. https://doi.org/10.1016/j.seta.2019.100586

Orlandi, A., Collu, M., Zanforlin, S., Shires, A., 2015. 3D URANS analysis of a vertical axis wind turbine in skewed flows. J. Wind Eng. Ind. Aerodyn. 147, 77–84.

https://doi.org/10.1016/j.jweia.2015.09.010

Rainbird, J., 2007. The aerodynamic development of a vertical axis wind turbine. MEng Proj. ReporSchool Eng. Univ. Durham, UK.

Saad, A.S., Elwardany, A., El-Sharkawy, I.I., Ookawara, S., Ahmed, M., 2021. Performance evaluation of a novel vertical axis wind turbine using twisted blades in multi-stage Savonius rotors. Energy Convers. Manag. 235, 114013. https://doi.org/10.1016/j.enconman.2021.114013

Sengupta, A.R., Biswas, A., Gupta, R., 2016. Studies of some high solidity symmetrical and unsymmetrical blade H-Darrieus rotors with respect to starting characteristics, dynamic performances and flow physics in low wind streams. Renew. Energy 93, 536–547. https://doi.org/10.1016/j.renene.2016.03.029

Sheldahl, R.E., Klimas, P.C., 1981. Aerodynamic characteristics of seven symmetrical airfoil sections through 180-degree angle of attack for use in aerodynamic analysis of vertical axis wind turbines.

Su, H., Dou, B., Qu, T., Zeng, P., Lei, L., 2020. Experimental investigation of a novel vertical axis wind turbine with pitching and self-starting function. Energy Convers. Manag. 217, 113012. https://doi.org/10.1016/j.enconman.2020.113012

Sun, X., Zhu, J., Hanif, A., Li, Z., Sun, G., 2020. Effects of blade shape and its corresponding moment of inertia on self-starting and power extraction performance of the novel bowl-shaped floating straight-bladed vertical axis wind turbine. Sustain. Energy Technol. Assessments 38, 100648. https://doi.org/10.1016/j.seta.2020.100648

Sun, X., Zhu, J., Li, Z., Sun, G., 2021. Rotation improvement of vertical axis wind turbine by offsetting pitching angles and changing blade numbers. Energy 215, 119177. https://doi.org/10.1016/j.energy.2020.119177

Syawitri, T.P., Yao, Y., Yao, J., Chandra, B., 2022. Geometry optimisation of vertical axis wind turbine with Gurney flap for performance enhancement at low , medium and high ranges of tip speed ratios. Sustain. Energy Technol. Assessments 49, 101779. https://doi.org/10.1016/j.seta.2021.101779

Tavallaeinejad, M., Fereidoooni, A., Païdoussis, M.P., Grewal, A., Wickramasinghe, V., 2022. An application of cantilevered plates subjected to extremely large amplitude deformations: A self-starting mechanism for vertical axis wind turbines. J. Fluids Struct. 113, 103666. https://doi.org/10.1016/j.jfluidstructs.2022.103666

Torabi, M., Zal, E., Mustapha, F., Wiriadidjaja, S., 2016. Study on start-up characteristics of H-Darrieus vertical axis wind turbines comprising NACA 4-digit series blade airfoils. Energy 112, 528–537. https://doi.org/10.1016/j.energy.2016.06.059

Ullah, T., Javed, A., Abdullah, A., Ali, M., Uddin, E., 2020. Computational evaluation of an optimum leading-edge slat deflection angle for dynamic stall control in a novel urban-scale vertical axis wind turbine for low wind speed operation. Sustain. Energy Technol. Assessments 40, 100748. https://doi.org/10.1016/j.seta.2020.100748

Wang, S., Ingham, D.B., Ma, L., Pourkashanian, M., Tao, Z., 2010. Numerical investigations on dynamic stall of low Reynolds number flow around oscillating airfoils. Comput. Fluids 39, 1529–1541. https://doi.org/10.1016/j.compfluid.2010.05.004

Yagmur, S., Kose, F., 2021. Numerical evolution of unsteady wake characteristics of H-type Darrieus Hydrokinetic Turbine for a hydro farm arrangement. Appl. Ocean Res. 110,

102582. https://doi.org/10.1016/j.apor.2021.102582

Yousefi Roshan, M., Khaleghinia, J., Eshagh Nimvari, M., Salarian, H., 2021. Performance improvement of Darrieus wind turbine using different cavity layouts. Energy Convers. Manag. 246, 114693. https://doi.org/10.1016/j.enconman.2021.114693

Zamani, M., Maghrebi, M.J., Varedi, S.R., 2016a. Starting torque improvement using J-shaped straight-bladed Darrieus vertical axis wind turbine by means of numerical simulation. Renew. Energy 95, 109–126. https://doi.org/10.1016/j.renene.2016.03.069

Zamani, M., Nazari, S., Moshizi, S.A., Maghrebi, M.J., 2016b. Three dimensional simulation of J-shaped Darrieus vertical axis wind turbine. Energy 116, 1243–1255. https://doi.org/10.1016/j.energy.2016.10.031

Zhang, T. tian, Elsakka, M., Huang, W., Wang, Z. guo, Ingham, D.B., Ma, L., Pourkashanian, M., 2019. Winglet design for vertical axis wind turbines based on a design of experiment and CFD approach. Energy Convers. Manag. 195, 712–726. https://doi.org/10.1016/j.enconman.2019.05.055

Zhao, Z., Wang, D., Wang, T., Shen, W., Liu, H., Chen, M., 2022. A review: Approaches for aerodynamic performance improvement of lift-type vertical axis wind turbine. Sustain. Energy Technol. Assessments 49, 101789. https://doi.org/10.1016/j.seta.2021.101789

Zhu, J., Huang, H., Shen, H., 2015. Self-starting aerodynamics analysis of vertical axis wind turbine. Adv. Mech. Eng. 7, 1–12. https://doi.org/10.1177/1687814015620968